Lab on a Chip

View Online
Dynamic Article Links

Cite this: DOI: 10.1039/c1lc20207c

www.rsc.org/loc

PAPER

# Real-time PCR of single bacterial cells on an array of adhering droplets

**Xu Shi, Liang-I Lin, Szu-yu Chen, Shih-hui Chao,* Weiwen Zhang and Deirdre R. Meldrum**

***Received 8th March 2011, Accepted 21st April 2011***
**DOI: 10.1039/c1lc20207c**



Real-time PCR at the single bacterial cell level is an indispensable tool to quantitatively reveal the heterogeneity of isogenetic cells. Conventional PCR platforms that utilize microtiter plates or PCR tubes have been widely used, but their large reaction volumes are not suited for sensitive single-cell analysis. Microfluidic devices provide high density, low volume PCR chambers, but they are usually expensive and require dedicated equipment to manipulate liquid and perform detection. To address these limitations, we developed an inexpensive chip-level device that is compatible with a commercial real-time PCR thermal cycler to perform quantitative PCR for single bacterial cells. The chip contains twelve surface-adhering droplets, defined by hydrophilic patterning, that serve as real-time PCR reaction chambers when they are immersed in oil. A one-step process that premixed reagents with cell medium before loading was applied, so no on-chip liquid manipulation and DNA purification were needed. To validate its application for genetic analysis, *Synechocystis* PCC 6803 cells were loaded on the chip from 1000 cells to one cell per droplet, and their 16S rRNA gene (two copies per cell) was analyzed on a commercially available ABI StepOne real-time PCR thermal cycler. The result showed that the device is capable of genetic analysis at single bacterial cell level with $C_q$ standard deviation less than 1.05 cycles. The successful rate of this chip-based operation is more than 85% at the single bacterial cell level.

## Introduction

Traditional microbiology studies are built on examination of a large amount of cells. This approach often masks the difference in individual cells/species, especially for low abundance species in the population.[1]

Microfabrication and microfluidic technologies have led to the rapid development of many miniaturized analytical chips which can perform analysis down to single-cell levels.[2,3] Microfabricated devices can integrate several steps like lysis and chemical analysis on a single miniaturized platform. Compared with conventional analytical methods, the miniaturized platforms have the advantages of reducing contamination,[4] enabling the simultaneous parallel analytical process and decreasing the amount of chemicals and enzyme consumed.[2] Due to the minimized sample dilution during the biochemical process, the small reaction volume is especially advantageous to single cell analysis.[5] In a new study, Zhang *et al.* demonstrated parallel real-time PCR with the sensitivity of about 1000 cDNA copies per 500 nL droplet produced using conventional photolithography.[6] In addition, only a low fraction (~1%) of bacteria species in natural environments have been cultivated,[7–9] thus the ability to study bacteria at a single-cell level will enable the investigation of microbe species for which the cultivation methods have not been established.[2,10] In one recent study, Marcy and colleagues[11] developed a microfluidic device that performed isolation, amplification and sequencing of individual TM7 cells from a mixed microbial community that inhabits human mouths. The results showed low abundance species which would be easily neglected under traditional approaches.

Microdevices have been successfully applied to perform parallel PCR at the single copy level.[12–17] These analyses are highly sensitive, but their analytes which typically are purified DNA are much simpler than the raw lysate of actual cell analyses. In addition, the process does not involve cell lysis which usually results in more complicated chemical composition and/or fluidic manipulation. These factors limit single-cell PCR to reach the single copy resolution. Single bacterial cell studies are more challenging than that for mammalian cells due to the small size and their tough cell-wall structure. Recent progresses on using microfluidic devices on single-cell PCR have focused on mammalian cells. The applications on single bacterial cells are rare. Ottesen *et al.*[10] used microfluidic digital PCR to amplify and analyze different genes obtained from single bacterial cells gathered from the environments. They used this device to identify bacteria in complex ecosystems and successfully reached the single molecular level resolution based on serial dilution and Poisson distribution. Zeng *et al.*[18] designed an emulsion generating microfluidic device that used the small droplets in oil as the reaction chambers. In this experiment, *E. coli* cells or isolated

*Center for Biosignatures Discovery Automation, Arizona State University, PO Box 876501, Tempe, AZ, USA. E-mail: joe.chao@asu.edu; Fax: +1 480 727 6588; Tel: +1 480 727 8277*

DNA were randomly seeded into the droplets with primer-adhered microspheres and real-time PCR reagents. By measuring the fluorescent emission of the PCR product in droplets using flow cytometry, they demonstrated that single-bacteria-resolution analysis can be achieved. However, all of these devices need complicated microfabrication or/and designs which required specific instruments. Very often these instruments or expertise for fabrication are not readily available for most biological laboratories, which has limited the application of these devices for single cell studies.

To make genetic analysis of single-bacterial cells more accessible for general biological laboratories, we developed a new chip-level device which involves only inexpensive and easily accessible equipment. This device contains an array of stationary, surface-adhering droplets immersed in oil as real-time PCR chambers. Mineral oil is used to isolate the droplets and prevent the aqueous solution from evaporation during thermal cycling. The dimensions and locations of the droplets are controlled by hydrophilic patterning on the glass substrate. The volume of each chamber is 5 μL on our current design, but can be smaller and the density of the droplets can be higher if using a customized thermal cycler that can scan dense PCR chamber arrays. In addition, the operation does not require off-chip DNA extraction or purification steps which will diminish the potential affection of downstream real-time PCR analysis, such as inhibition from lysis buffer which is used for off-chip DNA extraction. Although single-cell loading can also be easily achieved by serial dilution,[19] we used a micromanipulator to precisely load one bacterial cell per droplet to validate the sensitivity. Leveraged with a commercially available real-time PCR thermal cycler, we demonstrated that the device is capable of genetic analysis at the single bacterial cell level.

## Method

### Experimental setup

The presented chip is designed to be compatible with an off-the-shelf real-time PCR thermal cycler originally designed to work with conventional PCR tubes/plates. Our chip contains an array of surface-adhering droplets on a microscope cover slip, and all droplets are submerged under an open pool of mineral oil confined by a PDMS frame (Fig. 1a). Each droplet is isolated by mineral oil as a PCR reaction chamber and to prevent the droplets from evaporation and cross-contamination. The chip is optically compatible with the thermal cycler since all components such as mineral oil and droplets are transparent. The locations of the droplets are aligned with the wells of the heating block designed to hold PCR tubes, and the area of a droplet is of the same order as the top-view area of a PCR tube (Fig. 1b). Therefore, the existing fluorescence detection configuration can be directly applied to the use of the chip. A 0.42 mm thick brass plate was placed under the cover slip during thermal cycling to enhance heat transfer for better temperature uniformity on the chip. The cross-view of the chip in a typical real-time PCR thermal cycler is shown in Fig. 1b.

In order to implement single bacterial cell analysis, the reaction volume of each chamber was designed at 5 μL, in contrast to the typical 10–20 μL reaction volume using conventional PCR tubes. Droplets smaller than 5 μL tended to be too small for the real-time PCR thermal cycler to detect. The smaller volume reactions increase the local concentration of template so that the competition with contaminant or endogenously generated background such as primer dimers will be reduced thus providing more DNA polymerase molecules per template.[12,20,21]

### Chip fabrication

The procedure of producing a droplet array is derived from our previous work that isolates single bacteria in a droplet array.[19] The key fabrication process is to make a hydrophilic pattern that confines the aqueous droplets. In this study, we generated such patterns using Microscale Plasma Activated Templating (μPLAT), a technique that employs a stencil to expose air plasma only to designed areas to increase the hydrophilicity of surface.[22] The process of making this chip is illustrated in Fig. 2. In order to minimize contamination, all components and material used in this study were autoclaved and exposed to UV light for 15 minutes before experiment.

First, a μPLAT stencil made of a 2 mm thick PDMS sheet was adhered on a cover slip (Fig. 2a). A 3 × 4 array of 1/8 inch diameter holes was punched, with a 9 mm pitch between centers to align with real-time PCR thermal cycler. Hence, twelve droplets can be fit in a 35 mm × 50 mm cover slip (12-545-G,

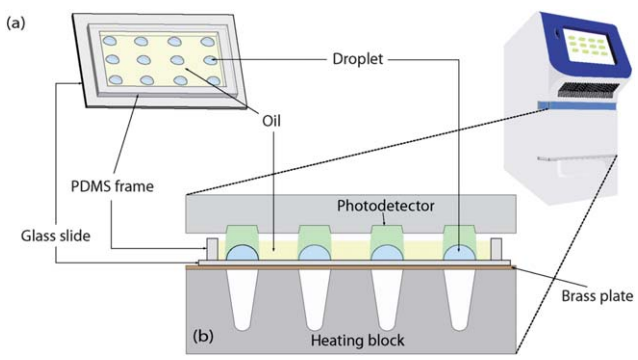


**Fig. 1** (a) The chip contains an array of surface-adhering droplets submerged in oil. (b) The cross-section view of the chip placed on a thermal cycler, showing that the droplets are aligned with the wells of the heating block of the thermal cycler (not to scale).

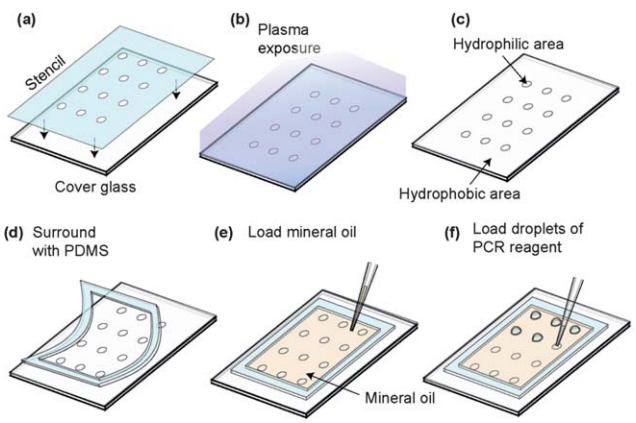


**Fig. 2** Chip fabrication process.

Fisher Scientific, Pittsburgh, PA). The soft PDMS stencil was then adhered on the cover slip. The assembly was placed in a plasma cleaner (PDC-32G, Harrick Plasma, Ithaca, NY) for plasma exposure with 6.8 W RF-power for one minute (Fig. 2b). The areas exposed to the plasma became more hydrophilic, while the unexposed areas remained unchanged. Then the stencil was removed, leaving an array of hydrophilic circular areas on a more hydrophobic background (Fig. 2c). A 2 mm thick PDMS frame was placed to surround the hydrophilic array to confine a pool of oil (Fig. 2d). 800 μL of mineral oil (Sigma M5904) was loaded inside the PDMS frame (Fig. 2e). Finally, twelve 5 μL droplets of PCR mixture were pipetted on each hydrophilic area (Fig. 2e). Oil was loaded before droplets to prevent the contamination to droplets from the environment during the loading process.

### Strain and cell culture

The *Synechocystis* PCC 6803 strain used in this study was obtained from American Type Culture Collection (ATCC). The *Synechocystis* PCC 6803 cells were grown at room temperature in BG-11 media at 30 °C.[23] The cell density of *Synechocystis* PCC 6803 was measured by a spectrophotometer (DU 530, Beckman Coulter, Brea, CA), and counted under a light microscope (Eclipse LV100, Nikon, Japan). In general, $OD_{730}$ 1.0 represents roughly $10^8$ cells per mL.

### Cell loading

Two cell loading approaches were used in the study. We used serial dilution to load averagely 1000, 100, and 10 cells per droplet. For single-cell loading, we used a single-cell micromanipulator developed in our center.[24,25] This micromanipulator uses a piezoelectric actuated diaphragm to dispense/aspirate liquid through a 30 μm capillary at the picolitre level. This device can precisely manipulate cells with small flow rates and therefore gentle shear stresses. The entire loading process was monitored on a microscope, so the loading of single bacteria cell can be visually confirmed.

### Real-time PCR

Primers were designed using Primer3 software[26] and manufactured by Invitrogen (Carlsbad, CA). One set of primers was designed to amplify a 152 bp of 16S rRNA gene of *Synechocystis* PCC 6803: forward primer (5′-CCACGCCTAGTATC CATCGT-3′) and reverse primer (5′-TGTAGCGGT GAAATGCGTAG-3′). The SYBR GreenER qPCR SuperMix Kit (Invitrogen, Carlsbad, CA) was used for real-time PCR. The PCR reaction mixture contained 2.5 μL qPCR SuperMix, 0.5 μL of each primer with the final concentration of 4 μM, 0.5 μL of 5 × BSA, 0.45 μL of DEPC treated water (Ambion, Austin, TX), 0.05 μL ROX and 0.5 μL sample in a total volume of 5 μL for each droplet. For a single cell droplet, 0.5 μL of DEPC treated water was loaded and then one single cell was put into the droplet using the micromanipulator. Considering the low fluorescent signal due to the low amount of target, photobleaching was prevented by blocking the ambient light. The experiments were performed on a commercially available thermal cycler (StepOne real-time PCR system, Applied Biosystems, Carlsbad, CA).

### PCR validation

After real-time PCR, the PCR products were pipetted out one by one and loaded on 1.5% agarose gels (EMD Chemical, Gibbstown, NJ) for electrophoresis analysis. The gels were run under 130 volts for 35 min. The DNA fragments with the expected size were then isolated using a QIAquick Gel Extraction Kit (QIAGEN, Valencia, CA) and analyzed by sequencing on ABI 3700. In order to confirm the right sequence, online nucleotide blast tools (http://blast.ncbi.nlm.nih.gov/) were used. Over 98% identity was recognized as right amplification. Validation is not necessary for regular utility of the device.

## Result and discussion

### PCR temperature profile

The efficiency and specificity of a PCR are affected by several factors, including cell lysis efficiency, chemical constitution of PCR system (*i.e.* primer concentration, $Mg^{2+}$ concentration, SYBR Green concentration, *etc.*) and annealing temperature.[27,28] For real-time PCR, the temperature at which fluorescence detection is performed is also a crucial factor.

Thermal lysis was selected over chemical lysis to avoid possible interference with PCR due to chemical lysing.[29–31] In this study, we found that heating at 94 °C for 10 minutes was enough to fully lyse the *Synechocystis* PCC 6803 cells in the droplets. Based on the sequence analysis and initial tests, 60 °C was found as the optimized annealing temperature, and was selected for the rest of the study.

SYBR green dye only binds to double-stranded DNA in a specific temperature range, so the fluorescence emission that indicates the quantity of double-stranded DNA can be detected. The proper detection temperature can be determined through the melt curve analysis. After testing from multiple temperatures ranged from 70 °C to 80 °C on chips, the optimized signal detection temperature was determined as 72 °C, and was selected for the rest of the study.

As shown in Fig. 1, the heat from the heating block of the thermal cycler transferred to the droplet through the air in the heating block. Since the droplets did not directly contact with the thermal cycler, the temperature of the droplets experienced offset and delay to the set temperature on the thermal cycler. To solve the issue, we focused our initial efforts on minimizing the difference in temperature related to each of the steps (*i.e.* cell lysis, annealing and signal detection) between the ideal temperatures and the real temperatures in droplets. The ideal temperature protocol for this study was 15 s at 95 °C for denaturing, 15 s at 60 °C for annealing, 30 s at 72 °C for extension, and 10 s at 72 °C for signal detection. In order to compensate the offset and hysteretic delay of the real temperature in the droplets, a calibration was performed by inserting a 0.076 mm diameter K-type thermocouple (5SC-TT-K-40-36, OMEGA) into the center of a droplet to empirically adjust the set temperatures and corresponding durations of the thermal cycler to fit the actual temperatures in the droplets. A thermocouple reader (50 Series II, Fluke) was used to record the temperature every five seconds during thermal cycling. Fig. 3 shows the temperature profile set on the thermal cycler (filled circles) and the compensated temperature profile in the droplets (line with rectangular dots).

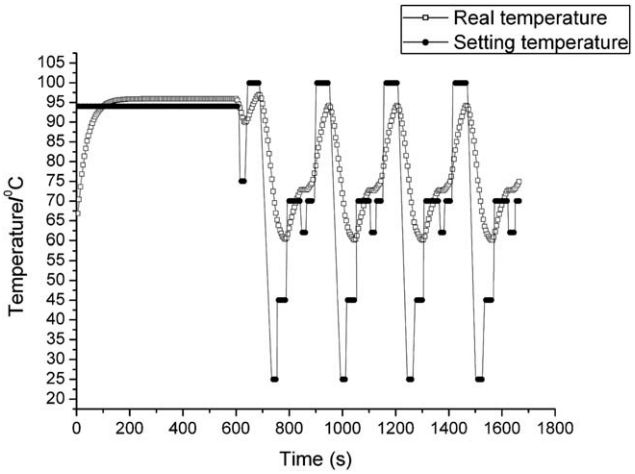


**Fig. 3** Temperature profile for PCR.

The heating/cooling rates were longer than those for conventional in-tube PCR, so the droplets required a longer time to reach a steady-state temperature. To shorten the total duration, we selected not to wait for the temperature at each stage to reach steady state. Instead, the thermal cycling profile was selected such that the droplet temperature was maintained within a ±1 °C range from the desire temperature during each stage.

## Single bacterial cell analysis

In order to accomplish the real-time PCR with a single digit template copy in single bacterial cells, in addition to the temperature profile, primer design is also a crucial factor.[32,33] The criteria for the primer design used in this study is that the size of the amplicon should be around 200 bp, $T_m$ value of the primers should be around 60 °C and several sets of primer need to be tested before choosing the right primers. Based on these requirements, the primers used in this study were designed by Primer3 (http://frodo.wi.mit.edu/primer3/). BSA was added in the solution to prevent undesired binding of DNA and polymerase to the glass surface.[34–37]

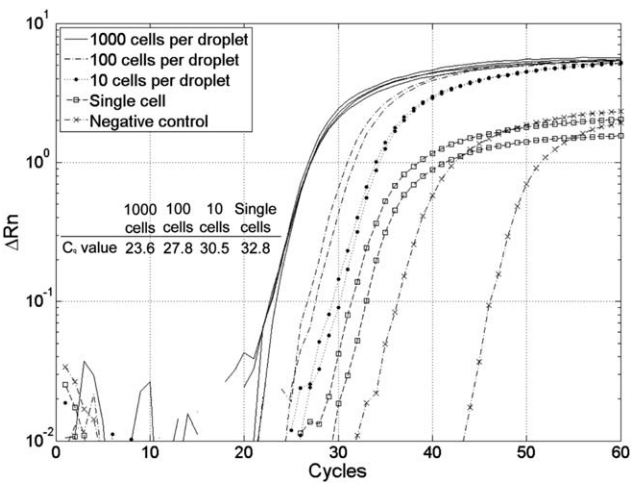


**Fig. 4** Real-time PCR results at 1000, 100, 10, and single cell levels.

The real-time amplification curves of an on-chip PCR experiment with various cell numbers are shown in Fig. 4. Four levels of cell number on the chip were tested. 1000, 100 and 10 cells per droplet were achieved by serial dilution from bulk cells, while single cells were picked and loaded directly with the micromanipulator. The average $C_q$ values were also shown in Fig. 4. The curves are well clustered for each cell number level. The differences in the average $C_q$ value between the cell number clusters were 4.2, 2.7 and 2.3, respectively. All amplified DNA was confirmed by sequencing as the expected products. Although the negative controls were frequently amplified in our experiments, they appeared significantly later than the reactions from single cells. In addition, the $T_m$ values of negative controls are different from that of the template. We also sequenced the amplification products from the negative control, and the BLAST search showed that the products were different and could be a result of random amplification (data not shown). The possible causes for the amplification of negative control are: (1) the contamination carried in commercial kits, enzyme and buffer, this contamination has been reported in many studies;[38,39] and (2) random amplification when the cycle number is high.

## Performance evaluation

In order to evaluate the performance of the chip, we first determined the successful rate of the chip operation. The melt curves were analyzed to define whether the reactions were successful. Briefly, each amplicon should have a specific $T_m$ value, then melt curves with dominant signal at the right $T_m$ value were recognized as a successful amplification. In addition, PCR products were validated through gel analysis and sequencing analysis. Based on these criteria, the overall successful rate from experiments shown in Fig. 4 and 5 was over 85% and the single cell level successful rate is at the same range.

The means and standard deviations of the $C_q$ values of different 16S rRNA template concentrations are summarized in Fig. 5. In these experiments, four different concentrations of

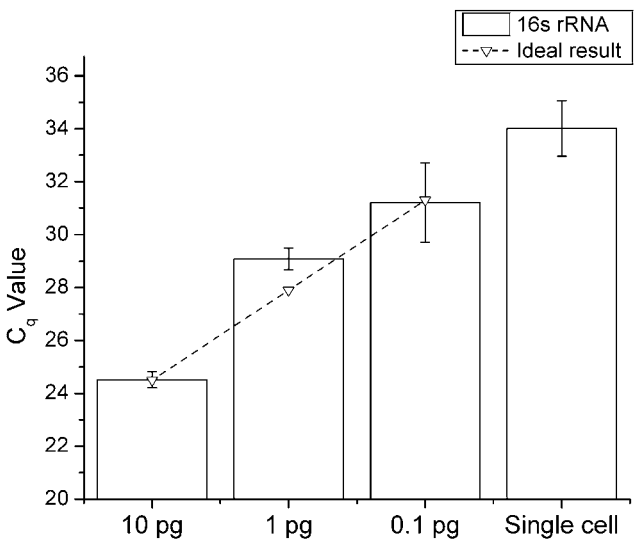


**Fig. 5** Template concentrations and $C_q$ values for on-chip PCR experiments.

template were loaded on four chips respectively. Each *Synechocystis* PCC 6803 cell contains femtogram-level DNA per cell,[40] so 10 pg DNA is equivalent to 1000 *Synechocystis* cells. The error bars of the $C_q$ are larger for lower concentrations, indicating that the reproducibility of the chip-based real-time PCR decreased as the template concentration decreased. One possible reason for the decreased reproducibility could be due to signal detection for the low amount of amplified DNA. Unexpected DNA binding to the glass surface may be another possible reason for the decreased reproducibility.

Between each 10× serial dilution, the ideal $C_q$ value difference is around 3.324 (*i.e.* $\log_2 10$) cycles. Our experimental results showed that the differences between each dilution level are 4.6 and 2.1 cycles between 10 pg and 1.0 pg and 1.0 pg and 0.1 pg dilutions, respectively, and 6.7 cycles between 10 pg and 0.1 pg dilutions. This result showed that although variations existed for individual experiments, the global trend of the relation between $C_q$ value and template concentration was close to the estimation with the ideal efficiency. We also designed another set of primers to amplify a 198 bp fragment of *rbcl* gene of *Synechocystis* PCC 6803. The $C_q$ difference between 10 pg and 1 pg was 3.2. The result confirmed that the PCR efficiency of our device was robust (data not shown).

In addition to successful rate and efficiency, sensitivity is another crucial factor for single bacterial cell study since the analyte amount is extremely low.[2,3,41] One *Synechocystis* PCC 6803 cell only has 2 copies of 16S rRNA gene, according to the NCBI and CyanoBase database (http://www.ncbi.nlm.nih.gov/gene; http://genome.kazusa.or.jp/cyanobase). Therefore, the sensitivity of the presented work approached the single copy level, similar to the sensitivities achieved with 6.25 nL microchambers[10] and 70 pL droplets[13] in previous works. However, because the droplet volume in our device was in μL scale, so our sensitivity in terms of initial template concentration is much higher. We assert that the one-step operation conserved the small number of templates in the confined droplet volume, and the reduction liquid transportation also minimized possible contamination which allowed for high thermal circle numbers with acceptable negative control expression. The elimination of DNA extraction and purification did not prevent quantitative analyses at low template concentration.

## Conclusion

In this study, a new design of an easily fabricated multi-chamber real-time PCR chip was demonstrated. The chip was robust and cost-efficient, and the one-step operation does not require DNA purification. The presented chip has the capability to analyze twelve single bacterial cells in one experiment, constrained by the commercial thermal cycler. Using the new device, we successfully extend qPCR analysis of the gene target toward the single copy level. Through serial dilution at low template concentration, statistics of $C_q$ values follows the ideal estimation. With the introduction of a specific designed thermal cycler for this platform in the future, the platform will have the capability to further decrease the reaction volume to nL level, similar to the other PCR microdevices that use non-adhering droplets as reaction chambers. The throughput and the sensitivity of the platform will be significantly increased. The application of this device in biological laboratories will provide the needed and convenient tools to perform genetic analysis for single bacterial cells and reveal heterogeneity in complex microbial communities. This technique is readily adaptable for analyzing mammalian cells.

## Acknowledgements

We gratefully acknowledge the support of this research by the NIH National Human Genome Research Institute, Grant Number 1 R01HG01497 Microscale Instrument Development for Genomic Analysis and ASU. We also appreciate Dr Weimin Gao for his assistance with primer design and Dr Yasser Anis for the micromanipulator.

## References

1 N. Musat, H. Halm, B. Winterholler, P. Hoppe, S. Peduzzi, F. Hillion, F. Horreard, R. Amann, B. B. Jørgensen and M. M. M. Kuypers, *Proc. Natl. Acad. Sci. U. S. A.*, 2008, **105**, 17861–17866.
2 R. N. Zare and S. Kim, *Annu. Rev. Biomed. Eng.*, 2010, **12**, 187–201.
3 A. Schmid, H. Kortmann, P. S. Dittrich and L. M. Blank, *Curr. Opin. Biotechnol.*, 2010, **21**, 12–20.
4 K. D. Dorfman, M. Chabert, J.-H. Codarbox, G. Rousseau, P. de Cremoux and J.-L. Viovy, *Anal. Chem.*, 2005, **77**, 3700–3704.
5 C. E. Sims and N. L. Allbritton, *Lab Chip*, 2007, **7**, 423–440.
6 Y. Zhang, Y. Zhu, B. Yao and Q. Fang, *Lab Chip*, 2011, **11**, 1545–1549.
7 R. I. Amann, W. Ludwig and K. H. Schleifer, *Microbiol. Rev.*, 1995, **59**, 143–169.
8 M. S. Rappé and S. J. Giovannoni, *Annu. Rev. Microbiol.*, 2003, **57**, 369–394.
9 N. R. Pace, *Science*, 1997, **276**, 734–740.
10 E. A. Ottesen, J. W. Hong, S. R. Quake and J. R. Leadbetter, *Science*, 2006, **314**, 1464–1467.
11 Y. Marcy, C. Ouverney, E. M. Bik, T. Lösekann, N. Ivanova, H. G. Martin, E. Szeto, D. Platt, P. Hugenholtz, D. A. Relman and S. R. Quake, *Proc. Natl. Acad. Sci. U. S. A.*, 2007, **104**, 11889–11894.
12 A. Musyanovych, V. Mailänder and K. Landfester, *Biomacromolecules*, 2005, **6**, 1824–1828.
13 N. R. Beer, B. J. Hindson, E. K. Wheeler, S. B. Hall, K. A. Rose, I. M. Kennedy and B. W. Colston, *Anal. Chem.*, 2007, **79**, 8471–8475.
14 F. Diehl, M. Li, Y. He, K. W. Kinzler, B. Vogelstein and D. Dressman, *Nat. Methods*, 2006, **3**, 551–559.
15 Y. Matsubara, K. Kerman, M. Kobayashi, S. Yamamura, Y. Morita, Y. Takamura and E. Tamiya, *Anal. Chem.*, 2004, **76**, 6434–6439.
16 T. Kojima, Y. Takei, M. Ohtsuka, Y. Kawarasaki, T. Yamane and H. Nakano, *Nucleic Acids Res.*, 2005, **33**, e150.
17 M. Nakano, J. Komatsu, S. Matsuura, K. Takashima, S. Katsura and A. Mizuno, *J. Biotechnol.*, 2003, **102**, 117–124.
18 Y. Zeng, R. Novak, J. Shuga, M. T. Smith and R. A. Mathies, *Anal. Chem.*, 2010, **82**, 3183–3190.
19 L.-I. Lin, S.-h. Chao and D. R. Meldrum, *PLoS One*, 2009, **4**, e6710.
20 Y. Marcy, T. Ishoey, R. S. Lasken, T. B. Stockwell, B. P. Walenz, A. L. Halpern, K. Y. Beeson, S. M. D. Goldberg and S. R. Quake, *PLoS Genet.*, 2007, **3**, 1702–1708.
21 Y. Schaerli and F. Hollfelder, *Mol. BioSyst.*, 2009, **5**, 1392–1404.
22 S. h. Chao, R. Carlson and D. R. Meldrum, *Lab Chip*, 2007, **7**, 641–643.
23 C. Richaud, G. Zabulon, A. Joder and J.-C. Thomas, *J. Bacteriol.*, 2001, **183**, 2989–2994.
24 Y. H. Anis, M. R. Holl and D. R. Meldrum, *IEEE Trans. Autom. Sci. Eng.*, 2010, **7**, 598–606.
25 Y. Anis, J. Houkal, M. Holl, R. Johnson and D. Meldrum, *Biomed. Microdevices*, 2011, DOI: 10.1007/s10544-011-9535-5.
26 A. Untergasser, H. Nijveen, X. Rao, T. Bisseling, R. Geurts and J. A. M. Leunissen, *Nucleic Acids Res.*, 2007, **35**, W71–W74.
27 R. Sipos, A. Szekely, M. Palatinszky, S. Revesz, K. Marialigeti and M. Nikolausz, *FEMS Microbiol. Ecol.*, 2007, **60**, 341–350.
28 P. Markoulatos, N. Siafakas and M. Moncany, *J. Clin. Lab. Anal.*, 2002, **16**, 47–51.

29 H. Lu, M. A. Schmidt and K. F. Jensen, *Lab Chip*, 2005, **5**, 23–29.
30 C. Lee, G. Lee, J. Lin, F. Huang and C. Liao, *J. Micromech. Microeng.*, 2005, **15**, 1215–1223.
31 L. C. Waters, S. C. Jacobson, N. Kroutchinina, J. Khandurina, R. S. Foote and J. M. Ramsey, *Anal. Chem.*, 1998, **70**, 158–162.
32 X. Wang and B. Seed, *Nucleic Acids Res.*, 2003, **31**, e154.
33 F. Pattyn, F. Speleman, A. De Paepe and J. Vandesompele, *Nucleic Acids Res.*, 2003, **31**, 122–123.
34 M. Höss and S. Pääbo, *Nucleic Acids Res.*, 1993, **21**, 3913–3914.
35 M. Höss, M. Kohn, S. Pääbo, F. Knauer and W. Schröder, *Nature*, 1992, **359**, 199–199.
36 C. Kreader, *Appl. Environ. Microbiol.*, 1996, **62**, 1102–1106.
37 A. R. Prakash, M. Amrein and K. V. I. S. Kaler, *Microfluid. Nanofluid.*, 2007, **4**, 295–305.
38 S. Zhou, Z. Hou, N. Li and Q. Qin, *J. Appl. Microbiol.*, 2007, **103**, 1897–1906.
39 G. Panicker, M. L. Myers and A. K. Bej, *Appl. Environ. Microbiol.*, 2004, **70**, 498–507.
40 S. Hahn, X. Y. Zhong, C. Troeger, R. Burgemeister, K. Gloning and W. Holzgreve, *Cell. Mol. Life Sci.*, 2000, **57**, 96–105.
41 L. M. Borland, S. Kottegoda, K. S. Phillips and N. L. Allbritton, *Annu. Rev. Anal. Chem.*, 2008, **1**, 191–227.



 